Articles

A Chromium-Diphosphine System for Catalytic Ethylene Trimerization: Synthetic and Structural Studies of Chromium Complexes with a Nitrogen-Bridged Diphosphine Ligand with *ortho*-Methoxyaryl Substituents

Theodor Agapie, Michael W. Day, Lawrence M. Henling, Jay A. Labinger,* and John E. Bercaw*

Arnold and Mabel Beckman Laboratories of Chemical Synthesis, California Institute of Technology, Pasadena, California 91125

Received July 19, 2005

To gain molecular-level insight into the important features of a chromium-diphosphine catalytic system for ethylene trimerization, the coordination chemistry of chromium with "PNP" ligands (PNP^{OMe} = (*o*-$MeOC_6H_4)_2PN(CH_3)P$(*o*-$MeOC_6H_4)_2$, $P^{t-Bu}N^{i-amyl}P^{OMe}$ = (2-MeO-4-*t*-$BuC_6H_3)_2PN$(*i*-amyl)P(2-MeO-4-*t*-$BuC_6H_3)_2$) has been explored. Chromium(0) carbonyl complexes have been synthesized by CO displacement with diphosphine. Oxidation of $Cr(CO)_4\{\kappa^2$-(P,P)-$(PNP^{OMe})\}$ with I_2, Br_2, and $PhICl_2$ generates the corresponding chromium(III) halide complexes. Chromium(III) complexes $CrCl_3\{(\kappa^3$-(P,P,O)-$(PNP^{OMe})\}$, $CrCl_3\{\kappa^3$-(P,P,O)-$(P^{t-Bu}N^{i-amyl}P^{OMe})\}$, and $CrCl_2(CH_3)\{\kappa^3$-(P,P,O)-$(PNP^{OMe})\}$ can be synthesized by metalation with $CrCl_3(THF)_3$ or $CrCl_2(CH_3)(THF)_3$. Reaction of $CrCl_3\{\kappa^3$-(P,P,O)-$(PNP^{OMe})\}$ with *o*,*o*′-biphenyldiyl diGrignard affords CrBr(*o*,*o*′-biphenyldiyl)$\{\kappa^3$-(P,P,O)-$(PNP^{OMe})\}$. Single-crystal X-ray diffraction studies show that the Cr−O and Cr−P distances can vary significantly as a function of metal oxidation state and the other ligands bound to chromium. Variable-temperature ^2H NMR spectroscopy studies of chromium(III) complexes supported by PNP ligands indicate fluxional behavior with the ether groups interchanging at higher temperatures. Low-temperature ^2H NMR spectra are consistent with solution structures similar to the ones determined in the solid state.

Introduction

The oligomerization of ethylene typically leads to a broad range of α-olefins, requiring fractional distillation to isolate individual α-olefins.[1] There is increasing interest in developing catalytic systems that give better selectivity toward desirable alkenes. One of the most commercially useful olefins is 1-hexene, a comonomer for the synthesis of linear low-density polyethylene (LLDPE). Several recent reports describe catalytic systems that trimerize ethylene to 1-hexene with high selectivity.[2−16] Some ethylene trimerization catalysts are based on titanium and tantalum,[5,9,16] but the most numerous and successful systems are based on chromium.[2−4,6−8,10−14]

Scheme 1

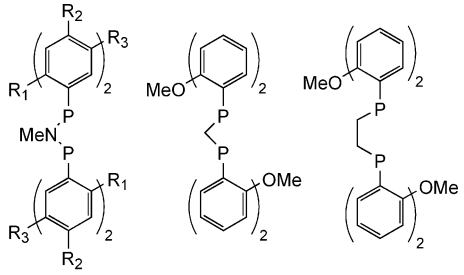

* **1**: R_1 = MeO, R_2 = R_3 =H **6** **7**
2: R_1 = Et, R_2 = R_3 = H
3: R_1 = R_3 = H, R_2 = MeO
* **4**: R_1 = R_3 = MeO, R_2 = H
* **5**: R_1 = MeO, R_2 = H, R_3 = F
* very active for ethylene trimerization

A catalyst generated from $CrCl_3(THF)_3$, a diphosphine ligand (**1**), and methaluminoxane (MAO) (eq 1) trimerizes ethylene to 1-hexene with unprecedented selectivity (99.9% 1-hexene in

(1) Skupinska, J. *Chem. Rev.* **1991**, *91*, 613.
(2) Briggs, J. R. *Chem. Commun.* **1989**, 674.
(3) Kohn, R. D.; Haufe, M.; Kociok-Kohn, G.; Grimm, S.; Wasserscheid, P.; Keim, W. *Angew. Chem., Int. Ed.* **2000**, *39*, 4337.
(4) Carter, A.; Cohen, S. A.; Cooley, N. A.; Murphy, A.; Scutt, J.; Wass, D. F. *Chem. Commun.* **2002**, 858.
(5) Andes, C.; Harkins, S. B.; Murtuza, S.; Oyler, K.; Sen, A. *J. Am. Chem. Soc.* **2001**, *123*, 7423.
(6) McGuinness, D. S.; Wasserscheid, P.; Keim, W.; Hu, C.; Englert, U.; Dixon, J. T.; Grove, C. *Chem. Commun.* **2003**, 334.
(7) Wu, F.-J. (Amoco Corporation) US 5,811,618, 1998.
(8) Reagen, W. K.; Pettijohn, T. M.; Freeman, J. W. (Philips Petroleum Company) US 5,523,507, 1996.
(9) Deckers, P. J. W.; Hessen, B.; Teuben, J. H. *Organometallics* **2002**, *21*, 5122.
(10) Bollmann, A.; Blann, K.; Dixon, J. T.; Hess, F. M.; Killian, E.; Maumela, H.; McGuinness, D. S.; Morgan, D. H.; Neveling, A.; Otto, S.; Overett, M.; Slawin, A. M. Z.; Wasserscheid, P.; Kuhlmann, S. *J. Am. Chem. Soc*. **2004**, 14712.
(11) McGuinness, D. S.; Wasserscheid, P.; Keim, W.; Morgan, D.; Dixon, J. T.; Bollmann, A.; Maumela, H.; Hess, F.; Englert, U. *J. Am. Chem. Soc.* **2003**, *125*, 5272.
(12) Overett, M. J.; Blann, K.; Bollmann, A.; Dixon, J. T.; Hess, F.; Killian, E.; Maumela, H.; Morgan, D. H.; Neveling, A.; Otto, S. *Chem. Commun.* **2005**, 622.
(13) Blann, K.; Bollmann, A.; Dixon, J. T.; Hess, F. M.; Killian, E.; Maumela, H.; Morgan, D. H.; Neveling, A.; Otto, S.; Overett, M. J. *Chem. Commun.* **2005**, 620.

10.1021/om050605+ CCC: $33.50 © 2006 American Chemical Society
Publication on Web 04/28/2006

Scheme 2

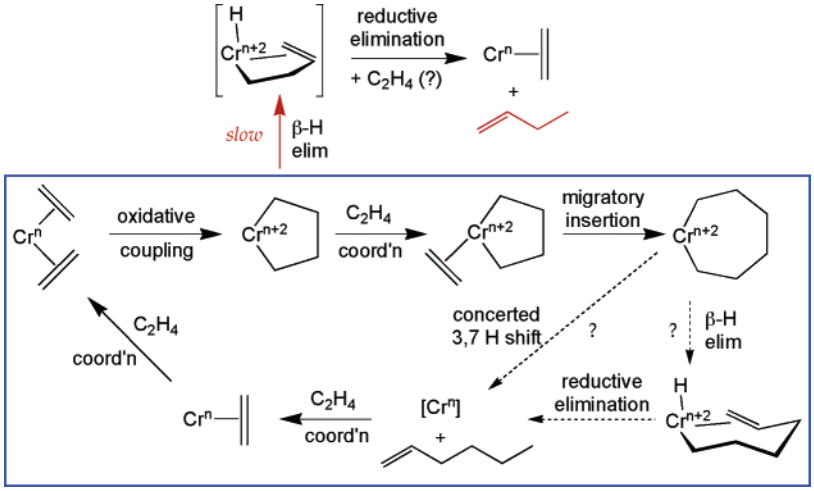

the hexenes fraction) and productivity (~2 × 10^6 turnovers/h).[4] The effect of changing the diphosphine on trimerization activity was investigated (Scheme 1); key features appear to be the *ortho*-methoxy-substituted aryl groups and the PNP backbone. Changing the amide in the PNP backbone to a methylene group (**6**) or replacing the *ortho*-methoxy groups with ethyl groups (**2**) greatly diminishes the catalytic activity. Recent studies involving a variety of related PNP ligands have shown that trimerization and tetramerization of ethylene can be achieved in the absence of *ortho*-donors, but these catalysts operate at higher pressures of ethylene and with lower selectivity for the terminal olefin in the corresponding C_n (n = 6 or 8) fraction.[10,12,13]

$$\text{ethylene} \xrightarrow[\text{300 equiv MAO, toluene}]{\text{CrCl}_3(\text{THF})_3 + \mathbf{1}} \text{1-hexene} \qquad (1)$$

Although details concerning the mechanisms of the trimerization (or tetramerization) reaction are not yet clear, the most popular proposed mechanism to account for the high selectivity involves metallacyclic intermediates (Scheme 2).[2,4,5,17] Initial coordination of 2 equiv of ethylene to a ligated Cr^n species followed by oxidative coupling forms a chromacyclopentane of oxidation state Cr^{n+2}. The transition state for β-hydrogen elimination from the chromacyclopentane leading to 1-butene is expected to be rather strained; hence, ring expansion by ethylene insertion dominates. The resulting chromacycloheptane is flexible enough to undergo rapid β-hydrogen elimination, giving a chromium-alkenyl-hydride species that reductively eliminates 1-hexene to regenerate Cr^n and closes the catalytic cycle. In agreement, Jolly and co-workers have reported well-characterized chromacyclopentane and chromacycloheptane complexes; the latter decomposes more readily and yields 1-hexene.[18] More recently, it has been suggested that the release of 1-hexene from the metallacycloheptane intermediate proceeds via a concerted 3,7-hydrogen shift with formal two-electron reduction of the metal.[17,19−22] We recently reported experimental support for the chromacyclic pathway and ruled out alternative

Scheme 3

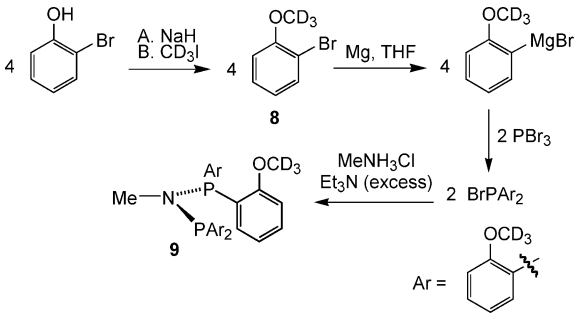

mechanistic possibilities such as a Cossee-type chain growth mechanism.[23] Further mechanistic investigations and synthetic work with related chromium complexes are expected to provide additional understanding of the important features of the Cr/PNP catalyst system.

We report herein the synthesis, characterization, and reactivity of chromium carbonyl, halide, alkyl, and aryl complexes supported by PNP ligands with *ortho*-methoxyaryl substituents. Part of this work was communicated previously.[23] The effects of varying the nature of the backbone linker atom and the *ortho*-substituents on the coordination chemistry of the diphosphine to chromium, their effects on the catalytic system, and mechanistic investigations of the ethylene trimerization and reactions with other olefins will be reported separately. A second study that describes closely analogous (PNP)chromium(III) phenyl derivatives appears in the following paper.[24]

Results and Discussion

Synthesis of PNP Ligands. ^{2}H NMR spectroscopy provides a valuable handle for the study of paramagnetic compounds.[25] Deuterium labeling can be achieved readily at the *ortho*-methoxyaryl position by methylating the appropriate phenol with CD_3I (Scheme 3). Two routes have been used for the synthesis of the diphosphine ligands (Schemes 3 and 4). For both routes ^{31}P NMR spectroscopy is a useful tool for monitoring the progress of the reaction. Scheme 3 outlines a linear protocol,

(14) McGuinness, D. S.; Wasserscheid, P.; Morgan, D. H.; Dixon, J. T. *Organometallics* **2005**, *24*, 552.
(15) Dixon, J. T.; Green, M. J.; Hess, F. M.; Morgan, D. H. *J. Organomet. Chem.* **2004**, *689*, 3641.
(16) Deckers, P. J. W.; Hessen, B.; Teuben, J. H. *Angew. Chem., Int. Ed.* **2001**, *40*, 2516.
(17) Yu, Z.-X.; Houk, K. N. *Angew. Chem., Int. Ed.* **2003**, *42*, 808.
(18) Emrich, R.; Heinemann, O.; Jolly, P. W.; Kruger, C.; Verhovnik, G. P. J. *Organometallics* **1997**, *16*, 1511.
(19) Blok, A. N. J.; Budzelaar, P. H. M.; Gal, A. W. *Organometallics* **2003**, *22*, 2564.
(20) de Bruin, T. J. M.; Magna, L.; Raybaud, P.; Toulhoat, H. *Organometallics* **2003**, *22*, 3404.
(21) Janse van Rensburg, W.; Grove, C.; Steynberg, J. P.; Stark, K. B.; Huyser, J. J.; Steynberg, P. J. *Organometallics* **2004**, *23*, 1207.
(22) Tobisch, S.; Ziegler, T. *Organometallics* **2003**, *22*, 5392.

Scheme 4

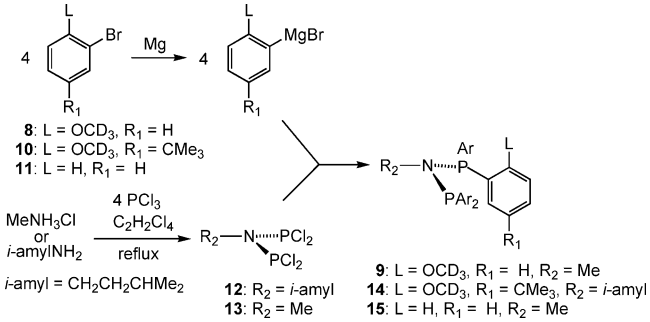

involving reaction of the Grignard reagent from deuterated 2-bromomethylphenyl ether (**8**) with PBr_3 to give bromodiarylphosphine.[26] Condensation with $(CH_3)NH_3Cl$ in the presence of excess tertiary amine provides the desired product. Even though this route could provide clean product in 60−70% yields, it was found that the last step was difficult to reproduce.

A convergent route was found to work well for the synthesis of a variety of PNP ligands (Scheme 4). This synthetic protocol takes advantage of the facile preparation of the PNP backbone unit (**12** or **13**),[27,28] which can be subsequently treated with a Grignard of choice (prepared from bromides such as **8**, **10**, or **11**) to give the desired diphosphines. Compound **14** was targeted as a more hydrocarbon-soluble version of **9**, as well as a system for comparison. During the last step in the preparation of **14**, intermediates such as the partially arylated species $(Ar_2PN(R^2)PArCl$ and $ArClPN(R^2)PArCl)$ were observed by ^{31}P NMR spectroscopy. It may be possible to use partially arylated species to obtain asymmetric diphosphines with both ligating (such as *o*-OMe) and nonligating (such as *o*-Et) aryl groups. An investigation of such a mixed ligand may provide information about the relation between the number of donors on the aryl groups and the catalytic activity.

Synthesis of $Cr(CO)_4\{(P,P)$-κ^2-$(PNP^{OMe})\}$ (16). Chromium(0) carbonyls provide a possible entry into chromium-diphosphine chemistry, and indeed, a chromium tetracarbonyl complex (**16**) supported by diphosphine **9** can be prepared readily starting from $Cr(CO)_6$ (eq 2). Spectroscopic data are consistent with a (P,P)-κ^2 coordination mode, without involvement of the ether groups. The average stretching frequency for the four CO normal modes is 1916 cm^{-1} (CH_2Cl_2) in **16**, about 10 cm^{-1} lower than those reported for $Cr(CO)_4\{(C_6H_5)_2PCH_2P(C_6H_5)_2\}$ or $Cr(CO)_4\{(C_6H_5)_2PCH_2CH_2P(C_6H_5)_2\}$ (~1927 cm^{-1}) (Table 1).[29] On the other hand, the average CO stretching frequency for the tetracarbonyl complex (**17**) supported by the PNP phosphine without ether substituents (**15**) is 1925 cm^{-1}, very similar to the values for $(C_6H_5)_2PCH_2P(C_6H_5)_2$ and $(C_6H_5)_2PCH_2CH_2P(C_6H_5)_2$. This suggests that the presence of more electron-rich aryl groups bearing ethers in **9** is the main reason for the greater electron density at the metal center in **16**.[30] The amide in the ligand backbone has a smaller effect.

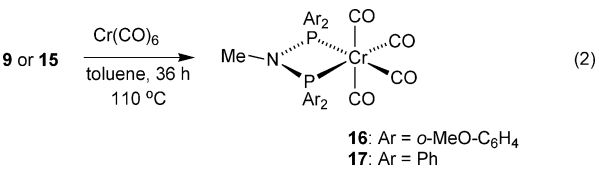

(2)

A single-crystal X-ray diffraction study confirmed the spectroscopic assignment of **16** (Figure 1). The Cr−P bond lengths are similar to the ones reported for analogous compounds.[31,32] Compared to $Cr(CO)_4(Me_2PCH_2PMe_2)$, **16** has a smaller P−Cr−P angle (67.54(2)° vs 70.78(3)°) and a larger P−N−P angle (101.24(7)° vs 95.74°) for P−C−P.[32]

Oxidation of $Cr(CO)_4\{(P,P)$-κ^2-$(PNP^{OMe})\}$: Accessing (PNP)chromium(III) Complexes. Considering that chromium(I)/chromium(III) is one of the possible redox couples performing the trimerization reaction (Scheme 2), chromium(III)- or chromium(I)-PNP complexes could furnish useful information regarding the relevant coordination chemistry of the catalyst and could provide good synthetic entries for mechanistic studies. The oxidation of **16** with $C_6H_5ICl_2$, Br_2, or I_2 affords $CrX_3(PNP^{OMe})$ (eq 3). The products with X = Cl (**18**) and I (**20**) were structurally characterized (Figures 2 and 3), confirming the structures shown with the PNP ligand bound in a κ^3-(P,P,O) fashion. While all the above products are paramagnetic (^2H NMR), diamagnetic byproducts are present as well in the crude reaction mixture. Recrystallization from CH_2Cl_2/petroleum ether mixture affords the desired chromium(III) products cleanly.

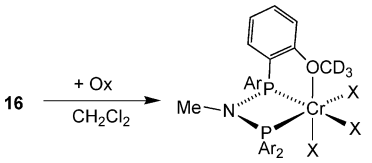

(3)

Synthesis of $CrCl_3\{\kappa^3$-(P,P,O)-$(PNP^{OMe})\}$ (18), $CrCl_3\{\kappa^3$-(P,P,O)-$(P^{t-Bu}N^{i-amyl}P^{OMe})\}$ (21), and $CrCl_2(CH_3)\{\kappa^3$-(P,P,O)-$(PNP^{OMe})\}$ (22) from Chromium(III) Starting Materials. Direct metallation with chromium(III) precursors provides an alternative pathway for the synthesis of PNP-supported chromium(III) complexes. Chromium(III) starting materials are commercially available ($CrCl_3(THF)_3$) or easy to prepare ($CrCl_2(CH_3)(THF)_3$),[33] facilitating the access to the complexes and their characterization (eq 4). Compounds **18**, **21**, and **22** were prepared by displacement of THF with the diphosphine ligand in CH_2Cl_2. Because coordinating solvents, such as THF, compete with the diphosphine for coordination to chromium(III), their use has been avoided or minimized. ^2H NMR spectroscopy is very useful in the characterization of the paramagnetic reaction products. Broad peaks downfield from the diamagnetic region indicate the formation of paramagnetic species.

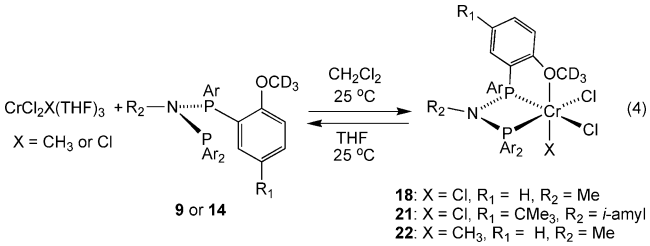

(4)

Solution magnetic susceptibility measurements obtained by the method of Evans[34,35] for the isolated compounds are

(23) Agapie, T.; Schofer, S. J.; Labinger, J. A.; Bercaw, J. E. *J. Am. Chem. Soc.* **2004**, *126*, 1304.
(24) Schofer, S. J.; Day, M. W.; Henling, L. M.; Labinger, J. A.; Bercaw, J. E. **2006**, *25*, 2743.
(25) La Mar, G. N.; Horrocks, W. D., Jr.; Holm, R. H. *NMR of Paramagnetic Molecules*; Academic Press: New York, 1973.
(26) Dossett, S. J.; Gillon, A.; Orpen, A. G.; Fleming, J. S.; Pringle, P. G.; Wass, D. F.; Jones, M. D. *Chem. Commun.* **2001**, 699.
(27) King, R. B.; Gimeno, J. *Inorg. Chem.* **1978**, *17*, 2390.
(28) Nixon, J. F. *J. Chem. Soc. A* **1968**, 2689.
(29) Gabelein, H.; Ellermann, J. *J. Organomet. Chem.* **1978**, *156*, 389.
(30) Tolman, C. A. *Chem. Rev.* **1977**, *77*, 313.
(31) Bennett, M. J.; Cotton, F. A.; LaPrade, M. D. *Acta Crystallogr.* **1971**, *B27*, 1899.

Table 1. Carbonyl Stretching Frequencies for Selected Complexes

	ν(CO) (CH_2Cl_2, cm^{-1})	$\nu(CO)_{av}$ (CH_2Cl_2, cm^{-1})
$Cr(CO)_4\{MeN(P(o\text{-}MeOC_6H_4)_2)_2\}$	2003, 1906, 1886, 1867	1916
$Cr(CO)_4\{MeN(PPh_2)_2\}$	2008, 1917, 1895, ~1881	1925
$Cr(CO)_4\{CH_2(PPh_2)_2\}$	2011, 1918, 1903, 1878	1927
$Cr(CO)_4\{C_2H_4(PPh_2)_2\}$	2011, 1917, 1903, 1878	1927

consistent with a quartet ground state ($\mu_{eff} = 3.8\ \mu_B$ for **18**, 3.9 μ_B for **21**, and 3.7 μ_B for **22**). Compounds **18** (Figure 3), **21** (see Supporting Information), and **22** (Figure 4) were structurally characterized by single-crystal X-ray diffraction; all display κ^3-(P,P,O) coordination of the diphosphine to yield a coordination number of six around the metal center. In **22**, the methyl group coordinates *trans* to the oxygen, rather than to the phosphorus, presumably due to a smaller *trans* influence for the ether donor. Due to the presence of a few disordered solvent molecules in the crystal, reliable structural parameters were not obtained for **21**; however, connectivity similar to **18** was observed. The fact that **18** and **21** have similar molecular structures may indicate that making changes at the periphery of the ligand (i.e., replacing a distal aryl-H with CMe_3 or replacing the N-methyl with N-*i*-amyl), while keeping the basic ligand framework constant (i.e., preserving the PNP backbone and *o*-ether-substituted aryls), does not substantially alter the binding mode of the methoxy-substituted diphosphine ligands. Comparisons among the structures of **18**, **20**, and **22** are presented in a later section.

Chromium Alkyls and Metallacyclopentanes as Entry Points for Mechanistic Studies: Synthesis of CrBr(*o*,*o*′-biphenyldiyl)$\{\kappa^3$-(P,P,O)-(PNP^{OMe})$\}$ (23). The proposed mechanism involves a chromacyclopentane intermediate;[18,36] isolation of such a complex could provide, upon activation, direct access to models of the species in the proposed catalytic cycle. Attempts to prepare analogues of metallacyclopentane have been successful, probably because chelation makes the products stable to side reactions. Compound **23** has been prepared from *o*,*o*′-biphenyldiyl Grignard reagent and chromium trichloride **18** (eq 5). The solid-state structure of **23** (Figure 5) shows distorted octahedral coordination with the biphenyldiyl group *trans* to

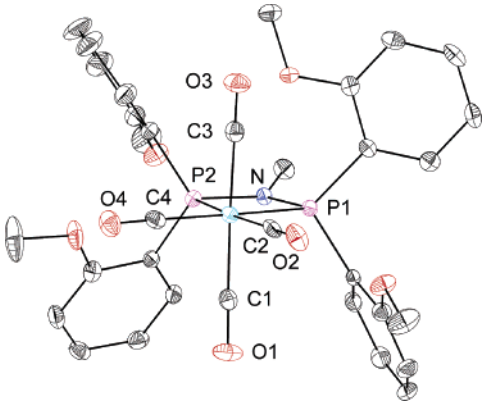

Figure 1. Structural drawing of **16** with displacement ellipsoids at the 50% probability level. Selected bond lengths (Å) and angles (deg): Cr−P_1 2.3557(6); Cr−P_2 2.3712(5); Cr−C_2,C_4 (av) 1.841; Cr−C_1,C_3 (av) 1.875; C_2−O_2,C_4−O_4 (av) 1.164; C_1−O_1,C_3−O_3 (av) 1.152; N−P_1 1.6946(14); N−P_2 1.7046(14); P_1−N−P_2 101.24(7); P_1−Cr−P_2 67.536(18).

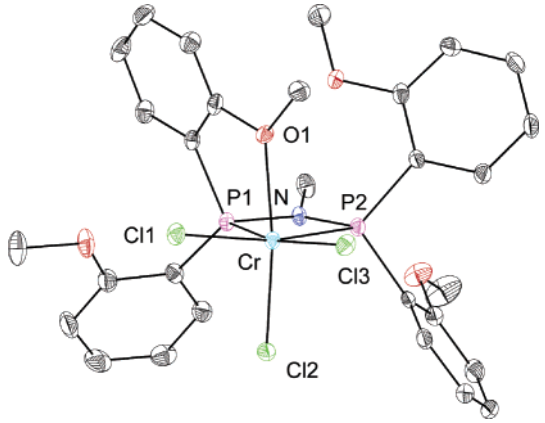

Figure 3. Structural drawing of **18** with displacement ellipsoids at the 50% probability level. Selected bond lengths (Å) and angles (deg): Cr−P_1 2.3855(7); Cr−P_2 2.5098(7); Cr−O_1 2.1562(15); Cr−Cl_1 2.2937(6); Cr−Cl_2 2.2776(6); Cr−Cl_3 2.3210(7); N−P_1 1.6920-(18); N−P_2 1.6978(18); P_2−Cr−P_1 66.56(2); O_1−Cr−Cl_2 165.62-(4); P_2−N−P_1 104.95(10).

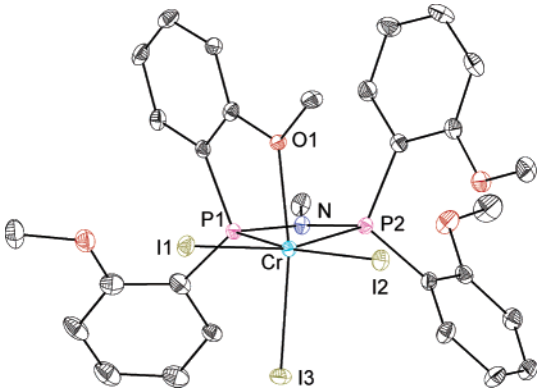

Figure 2. Structural drawing of **20** with displacement ellipsoids at the 50% probability level. Selected bond lengths (Å) and angles (deg): Cr−P_1 2.3891(6); Cr−P_2 2.5205(6); Cr−O_1 2.1820(14); Cr−I_1 2.6604(3); Cr−I_2 2.6765(3); Cr−I_3 2.6481(3); N−P_1 1.6990-(16); N−P_2 1.7020(16); P_2−Cr−P_1 66.825(18); O_1−Cr−I_3 163.77-(4); P_1−N−P_2 105.42(9).

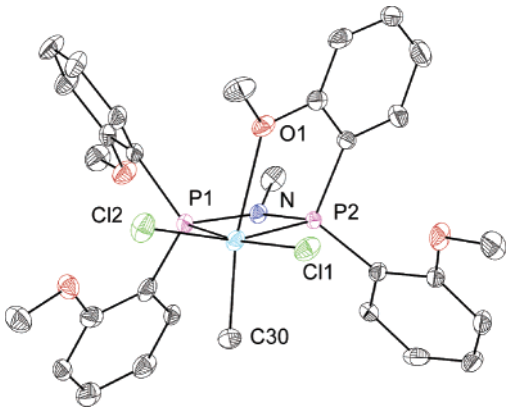

Figure 4. Structural drawing of **22** with displacement ellipsoids at the 50% probability level. Selected bond lengths (Å) and angles (deg): Cr−P_1 2.4010(10); Cr−P_2 2.5204(10); Cr−O_1 2.435(2); Cr−C_{30} 2.061(4); Cr−Cl_1 2.2939(10); Cr−Cl_2 2.3011(9); N−P_1 1.701-(2); N−P_2 1.691(3); P_2−Cr−P_1 66.54(3); O_1−Cr−C_{30} 166.44(15); P_1−N−P_2 105.58(14).

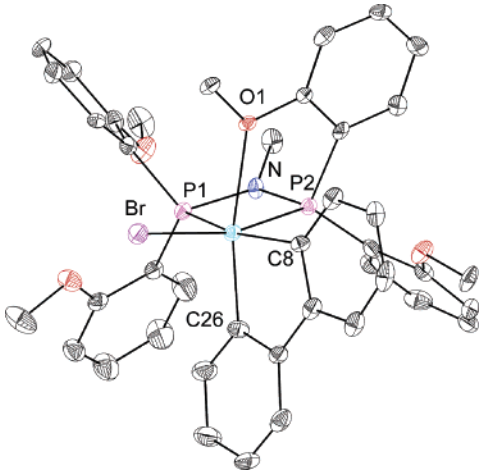

Figure 5. Structural drawing of **23** with displacement ellipsoids at the 50% probability level. Selected bond lengths (Å) and angles (deg): Cr−P_1 2.6606(14); Cr−P_2 2.4287(14); Cr−O_1 2.3331(33); Cr−C_{26} 2.0361(51); Cr−C_8 2.0611(49); Cr−Br 2.4811(9); N−P_1 1.7055(40); N−P_2 1.7049(38); P_2−Cr−P_1 64.97(4); C_{26}−Cr−C_8 82.04(21); P_1−N−P_2 106.93(19).

the weakly bound donors: the ether and the outside phosphine. The structure of **23** will be discussed in further detail in a later section. Bromide abstraction from **23** may be effected with Na[B(3,5-$(CF_3)_2$-$C_6H_3)_4$] in order to access a cationic chromium *o*,*o*′-biphenyldiyl complex. Although reaction occurred readily, giving one major product as assessed by ^{2}H NMR spectroscopy, its structure has not yet been fully characterized.

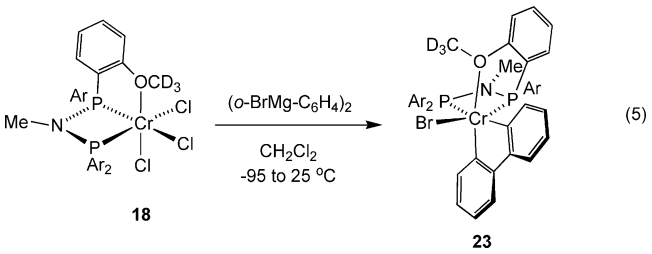

18 **23** (5)

The structures of **18**, **21**, and **22** show κ^3-coordination mode of the ligand. Since MAO is commonly used to generate a cationic transition metal alkyl from halide precursors, the active species in the proposed catalytic cycle (Scheme 2) may be a cationic chromium(III) dialkyl complex with one or more additional ether groups coordinated. Halide abstraction reactions from **18** and **22** occur readily, even with mild reagents such as Na[B(3,5-$(CF_3)_2$-$C_6H_3)_4$], but the resulting species have not been structurally characterized. Preparations of alkyl complexes, starting from **18**, **21**, and **22** and alkylating agents such as Grignard reagents and lithium, aluminum, and zinc alkyls, have been attempted, but have been unsuccessful thus far. An alternative route to (PNP)Cr-phenyl complexes is reported in the following article.[24]

Ether Exchange Processes in Complexes Supported by PNP Ligands. ^{2}H NMR spectroscopy proved to be instrumental in understanding the solution behavior of the (PNP)chromium(III) complexes. The number of peaks observed in the ^{2}H NMR spectra of all reported compounds is smaller than expected for the static solid-state structure. This suggests a dynamic process that allows the exchange of ether groups, and a variable-temperature ^{2}H NMR study was therefore undertaken (Figure 6).

Table 2. Coalescence Temperatures for Compounds 18, 21, 22, and 23 in CH_2Cl_2

	1st coalescence (°C)	2nd coalescence (°C)
18	−50	−10
21	−5	18
22	<−80	40[a]
23	−10	15

[a] In chlorobenzene.

Compounds **18**−**23** display one peak in the ^{2}H NMR spectra at the fast exchange limit (temperatures higher than 40 °C). Upon cooling, two decoalescence processes are apparent (Table 2). At the lowest temperatures one broad, presumably paramagnetically shifted peak corresponding to one ether and one (or two for **23**) sharper peak(s) is observed (Figure 6). At intermediate temperatures two peaks in a one-to-one ratio of intensities are observed, one broader and more paramagnetically downfield shifted (Figure 6, −25 °C spectrum and Figure 7).

The proposed processes that allow the stepwise, dynamic exchange of the ether groups are shown in Schemes 5 and 6 for compounds **18** and **22**. The lower barrier corresponds to uncoordination of the ether group, allowing two sets of two ether groups to interchange. The higher barrier corresponds to Berry pseudorotations that exchange the "top" and "bottom" of the molecule. In the case of complex **18**, only one Berry pseudorotation is necessary for this exchange (Scheme 5), while complex **22** requires three such processes (Scheme 6). Thus, at the highest temperatures, where this barrier is overcome, the ^{2}H NMR spectra display only one peak corresponding to fast interchange of the ether groups (Figure 6, 17 °C and 40 °C spectra). Similar variable-temperature behavior was observed for compounds **21** and **23**, indicating that ether exchange occurs in a variety of related complexes displaying different anionic ligands and peripheral ligand framework. The overlap of the noncoordinated ether signals even at low temperature (Figure 6, 60 °C spectrum) is probably due to smaller paramagnetic shifts and, hence, a smaller difference in their chemical shifts along with a broadening of the peaks due to the sample paramagnetism and increased viscosity.

Quantifying the thermodynamic barriers, for example by fitting the chemical shifts and/or line widths to predicted values, was not attempted, due to paramagnetic contributions in broadening and chemical shift. However, a qualitative analysis of some of the factors that could influence those energies suggests that the relative size of the barriers may correlate with the differences in the coalescence temperatures. For instance, comparing **18** and **22**, the first barrier is expected to be lower in **22** because of the stronger *trans* influence of the methyl group (ground state destabilized). The second barrier is expected to be higher in **22** because that process involves placing a methyl rather than a chloride *trans* to a phosphine (intermediate destabilized, more than the ground state).

Structural Comparisons between Cr/PNP^{OMe} Complexes. In all the characterized compounds, the metal center is six-coordinate. Moving from chromium(0) to chromium(III), the Cr−P bond lengths increase significantly (Table 3). The same general trend was found for other reported chromium(0) and chromium(III) complexes.[31,32,37−39] This may be due to a

(32) Jones, P. G.; Jager, S. *Z. Kristallogr.* **1997**, *212*, 85.
(33) Nishimura, K.; Kuribayashi, H.; Yamamoto, A.; Ikeida, S. *J. Organomet. Chem.* **1972**, *37*, 317.
(34) Sur, S. K. *J. Magn. Reson.* **1989**, *82*, 169.
(35) Evans, D. F. *J. Chem. Soc.* **1959**, 2003.
(36) Theopold, K. H. *Eur. J. Inorg. Chem.* **1998**, 15.
(37) Arif, A. M.; Jones, R. A.; Hefner, J. G. *J. Crystallogr. Spectrosc. Res.* **1986**, *16*, 673.

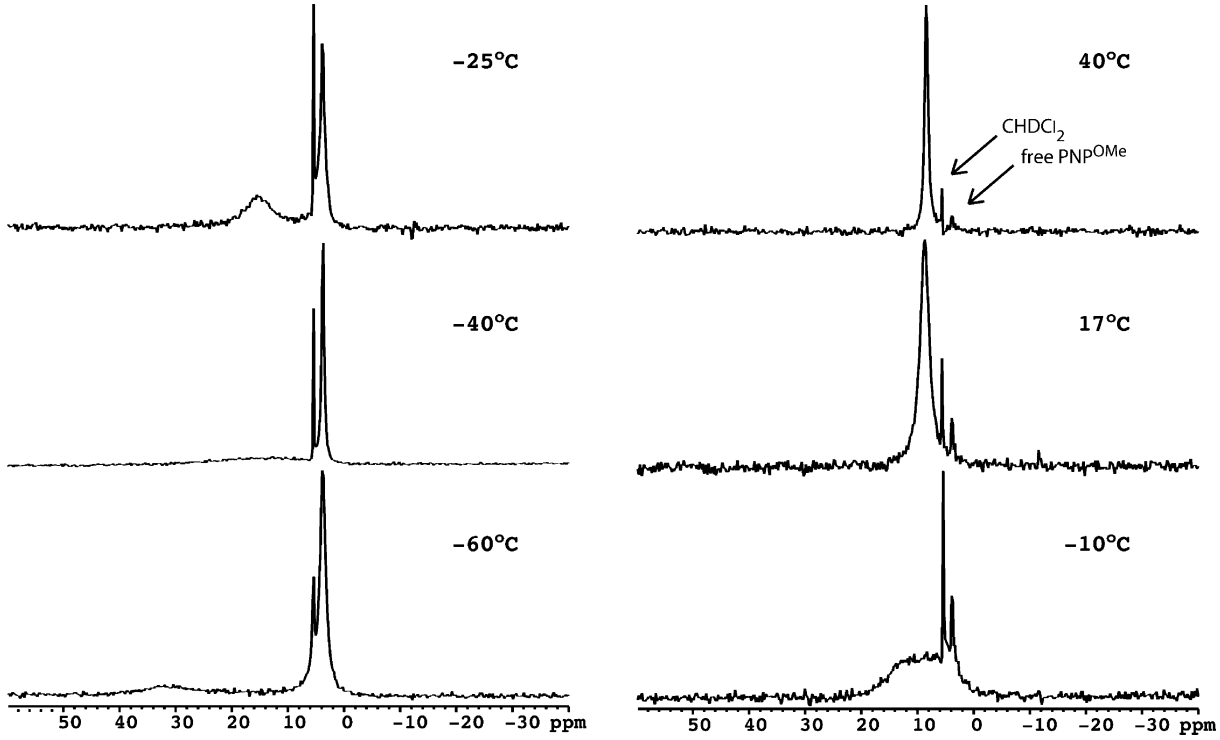

Figure 6. Variable-temperature ^{2}H NMR (CH_2Cl_2) spectroscopic study of **18**.

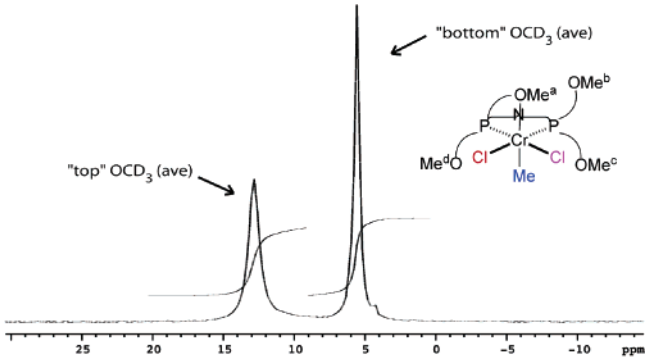

Figure 7. Room-temperature ^{2}H NMR (CH_2Cl_2) spectrum of **22**.

mismatch between the hard chromium(III) center and the soft phosphines, which counterbalances the contraction of the metal in the higher oxidation state. The P−Cr−P and P−N−P angles are each quite similar for the reported compounds; the most notable difference is in the P−N−P angle for chromium(0) versus chromium(III).

The two Cr−P bond lengths in all the chromium(III) compounds are significantly different, with Cr−P_b (P_b corresponds to the phosphine whose pendant ether coordinates to the metal) being shorter due to oxygen chelation. In the compounds containing homoleptic anionic ligand sets, the difference between the two Cr−P bond lengths is quite constant, between 0.12 (in **18**) and 0.14 Å (in $CrPh_3(PNP^{OMe})$).[23] The halide complexes show similar Cr−P as well as Cr−O bond lengths. Compared to the halide complexes, $CrPh_3(PNP^{OMe})$ shows elongation of all the Cr−PNP^{OMe} contacts, probably due to an increased *trans* influence from the phenyl groups.

When the anionic ligand sets are heteroleptic, the differences in structural parameters are more substantial. For instance, replacement of a chloride (in **18**) with a methyl (in **22**) leads to Cr−O bond elongation by almost 0.3 Å, likely due to a strong *trans* influence from the methyl group. The effect on the Cr−P bond lengths is small (<0.02 Å), suggesting that the PPO framework is quite flexible, so that each donor is able to adjust its distance to chromium without affecting the others significantly. In **23**, the presence of two different ligands (halide and aryl) in the P−Cr−P plane causes a larger difference between the two Cr−P bond lengths (∼0.23 Å). The Cr−P_b bond *trans* to the aryl groups elongated to 2.6606(14) Å, the longest Cr−P bond length to our knowledge.[40] The relatively small increase of the P−N−P angle and decrease of the P−Cr−P angle from **18** to **23** correlate with the increase in the Cr−P bond lengths, probably to minimize the overall ring deformation. Since the species involved in the catalytic cycle are presumably chromium alkyls, it is important to note that the methyl in **22** prefers to ligate *trans* to the ether, not to the phosphine, and that the *o*,*o*′-biphenyldiyl in **23** prefers to ligate *trans* to a phosphine and an ether rather than two phosphines.

Trimerization Trials with Well-Defined (PNP)chromium(III) Precursors. With (PNP)chromium(III) complexes in hand, ethylene trimerization tests were performed. Chromium complexes **18**, **21**, and **23** were activated with excess methyl aluminoxane (MAO, 300 equiv) in toluene under ethylene to generate systems active for catalytic ethylene trimerization (see the Supporting Information). The catalysts generated under these conditions are not stable catalyst systems, however, and ethylene trimerization activity decreases to ∼10% of the initial value within 30 min. Considering that the large excess of MAO hinders the utilization of ^{1}H NMR spectroscopy for mechanistic studies, stoichiometric activators have been investigated as well. It has been found that compound **23** can trimerize ethylene catalytically upon activation with $Na[B(3,5\text{-}(CF_3)_2\text{-}C_6H_3)_4]$. When **23** is exposed to ethylene without halide abstraction, no 1-hexene formation is observed (^{1}H NMR). This may be due

(38) Gray, L. R.; Hale, A. L.; Levason, W.; McCullough, F. P.; Webster, M. J. *J. Chem. Soc., Dalton Trans.* **1984**, 47.

(39) Gardner, T. G.; Girolami, G. S. *J. Chem. Soc., Dalton Trans.* **1987**, 1758.

(40) Cotton, F. A.; Duraj, S. A.; Powell, G. L.; Roth, W. J. *Inorg. Chem. Acta* **1986**, *113*, 81.

Scheme 5

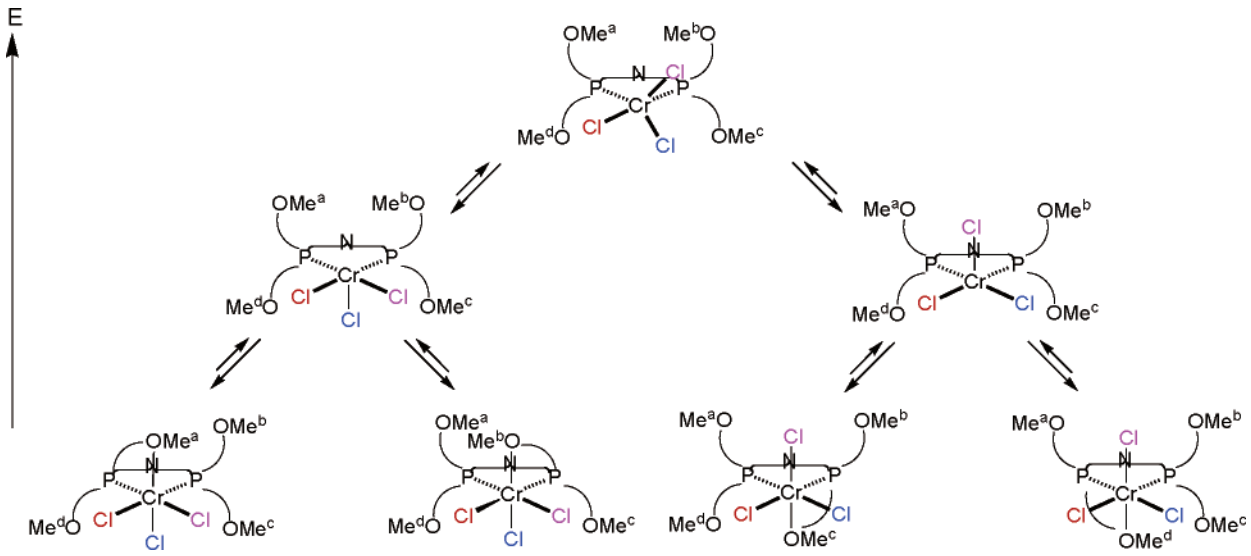

Scheme 6

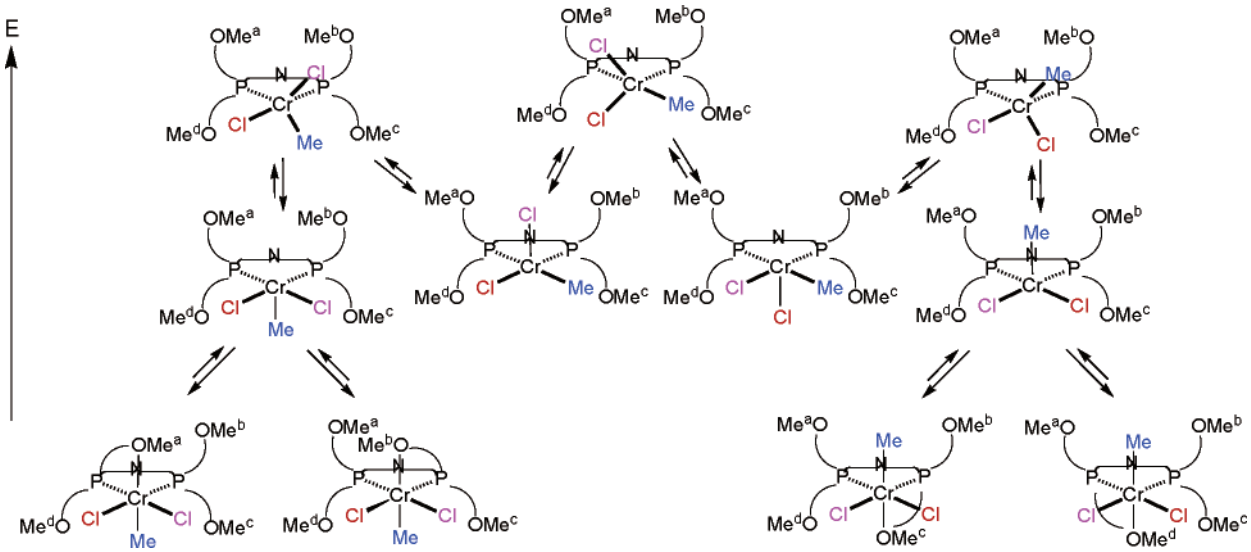

Table 3. Selected Structural Parameters for 16, 18, 20, Cr(PNP^{OMe})Ph$_3$, 22, and 23

	Cr−P$_a$ (Å)[a]	Cr−P$_b$ (Å)	Cr−O (Å)	P−N−P (deg)	P−Cr−P (deg)
16	2.3712(5)	2.3557(6)		101.24(7)	67.54(2)
18	2.5098(7)	2.3855(7)	2.1562(15)	104.95(10)	66.56(2)
20	2.5205(6)	2.3891(6)	2.1820(14)	105.42(9)	66.83(2)
CrPh$_3$(PNP^{OMe})[b]	2.6381	2.4971	2.286	105.72	64.02
22	2.5204(10)	2.4010(10)	2.435(2)	105.58(14)	66.54(3)
23	2.6606(14)	2.4287(14)	2.3331(33)	106.93(19)	64.97(4)

[a] P$_a$ corresponds to the outside phosphine (not chelated through an ether). [b] Average for the two molecules in the asymmetric unit.

to various factors including decreased electrophilicity or a smaller number of coordination sites available to an incoming olefin in the neutral complex.

Conclusions

A series of chromium(0) and chromium(III) complexes supported by PNP ligands have been synthesized and characterized. It has been found that the PNP ligand can display κ^2-(P,P) and *fac*-κ^3-(P,P,O) coordination modes. In all the cases investigated, a coordination number of six is observed for the chromium(III) center. The Cr−O bond length is very dependent (2.16 to 2.44 Å) on the nature of the ligand *trans* to the ether. Coordination of the pendant ether draws the corresponding phosphorus donor ca. 0.12−0.23 Å closer to Cr. One of the halide ligands is found to be labile in chromium(III)(PNP^{OMe}) complexes, facilitating the generation of cationic species. This has allowed the generation of a catalytic system for ethylene trimerization based on a chromium(III)(PNP^{OMe}) biphenyldiyl complex upon activation with stoichiometric amounts of Na[B(3,5-(CF$_3$)$_2$-C$_6$H$_3$)$_4$]. Activation of well-defined precursors with excess MAO also generates systems active for catalytic trimerization of ethylene. ^{2}H NMR spectroscopy has been very useful for the characterization of paramagnetic compounds. Variable-temperature ^{2}H NMR spectroscopy studies indicate

that, in solution, the ether groups are involved in a dynamic exchange process.

Experimental Section

General Considerations. All air- and moisture-sensitive compounds were manipulated using standard vacuum line, Schlenk, or cannula techniques or in a drybox under a nitrogen atmosphere. Solvents for air- and moisture-sensitive reactions were dried over sodium benzophenone ketyl or calcium hydride, or by the method of Grubbs.[41] Compound **13**[27,28] and $CrCl_2(CH_3)(THF)_3$[33] were prepared as described previously. Dichloromethane-d_2 was purchased from Cambridge Isotopes and distilled from calcium hydride. Other materials were used as received. Methylaluminumoxane was purchased from Aldrich. UV−vis measurements were taken on a Hewlett-Packard 8452A diode array spectrometer using a quartz crystal cell. Elemental analyses were performed by Desert Analytics, Tucson, AZ, and by Midwest Microlab, Indianapolis, IN. ^{1}H and ^{13}C NMR spectra were recorded on Varian Mercury 300 or Varian INOVA-500 spectrometers at room temperature, unless indicated otherwise. Chemical shifts are reported with respect to internal solvent: 5.32 (t) ppm and 54.00 (t) ppm (CD_2Cl_2); 7.27 ppm (s) and 77.23 ppm (t) ($CDCl_3$) for ^{1}H and ^{13}C data. ^{2}H NMR spectra were recorded on a Varian INOVA-500 spectrometer; the chemical shifts are reported with respect to an external D_2O reference (4.8 ppm). ^{31}P chemical shifts are reported with respect to an external H_3PO_4 85% reference (0 ppm).

Diphosphine Synthesis: Procedure 1.[42] Compound **8** (8.36 g, 44 mmol, 4 equiv) in tetrahydrofuran (THF, 100 mL) was added to magnesium turnings (1.32 g, 55 mmol, 5 equiv) using a pressure-equalizing funnel. The reaction mixture was stirred at 40 °C for ∼12 h. After cooling to room temperature, excess Mg was removed by filtration and the filtrate was added to a cold (−78 °C) solution of PBr_3 (2.09 mL, 22 mmol, 2 equiv) in THF (total volume ∼300 mL). After stirring for 1 h at low temperature, the mixture was allowed to reach room temperature and stir for 6 h (^{31}P NMR (121 MHz) of PAr_2Br δ: 63.2). NEt_3 (17 mL) was vacuum transferred to the reaction mixture followed by solid $MeNH_3Cl$ (0.743 g, 11 mmol, 1 equiv). The resulting mixture was stirred at room temperature overnight. Volatiles were removed under vacuum, and MeOH (70 mL) was added. The resulting slurry was cannula transferred to a sintered glass funnel, and the desired product **9** was collected by filtration (3.7 g, 7 mmol, 63% yield). ^{1}H NMR (300 MHz, $CDCl_3$) δ: 2.43 (t, $^3J_{HP}$ = 3.3 Hz, 3H, NCH_3), 3.61 (s, 12H, OCH_3, unlabeled version), 6.86 (app t, 8H, aryl-*H*), 7.07−7.11 (m, 4H, aryl-*H*), 7.31 (td, 4H, aryl-*H*). ^{13}C NMR (75 MHz, $CDCl_3$) δ: 33.9 (t, $^2J_{CP}$ = 5.7 Hz, NCH_3), 55.2 (OCH_3), 110, 120.1, 127.0 (t), 130, 133 (t), 160.7 (t). ^{31}P NMR (121 MHz, $CDCl_3$) δ: 52.2.

Diphosphine Synthesis: Procedure 2. Compound **8** (7.14 g, 37.6 mmol, 4 equiv) was added via syringe to a mixture of magnesium turnings (1.21 g, 50 mmol, 5.2 equiv) and tetrahydrofuran (40 mL). The reaction mixture was stirred at 50 °C for ∼12 h. After cooling to room temperature, excess Mg was removed by filtration. The filtrate was added to a THF solution of **13** (2.19 g, 9.4 mmol, 1 equiv). The transfer was completed with the aid of some THF (total solution volume ∼250 mL). The reaction mixture was stirred at 60 °C for ∼18 h. The reaction mixture was quenched with water and extracted with CH_2Cl_2. The combined organic fractions were dried over $MgSO_4$ and then filtered. Volatile materials were removed via rotary evaporation. The residue was dissolved in CH_2Cl_2, and half a volume of methanol was added. Upon concentration under vacuum, a white solid precipitated out and was collected by filtration. This procedure afforded 4.26 g (8 mmol, 85% yield) of spectroscopically pure desired product **9**.

(*i*-amyl)NPCl$_2$ (12). Compound **12** was synthesized using the published procedure used for **13**.[27,28] A mixture of *i*-amylamine (5 mL, 43 mmol, 1 equiv), PCl_3 (15 mL, 172 mmol, 4 equiv), and $C_2H_2Cl_4$ (30 mL) was refluxed, under argon, in an oil bath maintained at 150 °C. After 21 h the temperature was increased to 165 °C, and the mixture was refluxed for an additional 48 h. Then, the reaction mixture was allowed to cool and the desired product was collected by low-pressure distillation (60 °C, 0.03 Torr) as a colorless liquid, analytically pure by NMR spectroscopy (6.12 g, 51% yield). ^{1}H NMR (300 MHz, C_6D_6) δ: 0.73 (d, 6H, CH_3), 1.31 (nonet, 1H, $(CH_3)_2CHCH_2$), 1.64 (m, 2H, CHCH_2), 3.56 (m, 2H, NCH_2). ^{13}C NMR (75 MHz, C_6D_6) δ: 22.7, 27.3, 41, 47.7 (t, $^2J_{CP}$ = 4.9 Hz, NCH_2). ^{31}P NMR (121 MHz, $CDCl_3$) δ: 166.25.

(2-MeO-4-*t*-BuC$_6$H$_3$)$_2$PN(*i*-amyl)P(2-MeO-4-*t*-BuC$_6$H$_3$)$_2$, P^{t-Bu}N^{i-amyl}P^{OMe} (14). Procedure 2 was employed: 38% isolated yield. ^{1}H NMR (300 MHz, C_6D_6) δ: 0.59 (d, 6H, CH(CH_3)$_2$), 1.75 (br m, 2H, CHCH_2), 1.23 (s, 36H, C(CH_3)$_3$), 3.75 (br m, 2H, NCH_2), 6.58 and 7.23 (app d, 8H, aryl-*H*), 7.76 (app s, aryl-*H*). ^{13}C NMR (75 MHz, C_6D_6) δ: 23.4, 27.8, 32.1, 34.7, 41.2 (t, $^3J_{CP}$ = 3.9 Hz, NCH_2CH_2), 53.9 (t, $^2J_{CP}$ = 11.1 Hz, NCH_2), 110.7, 126.8, 129.5 (t), 132.1 (t), 142.9, 159.9 (t). ^{31}P NMR (121 MHz, C_6D_6) δ: 44.7. If the last step in the preparation of **14** is performed at room temperature, intermediates are observed by ^{31}P NMR spectroscopy (121 MHz, $CDCl_3$) δ: 138 (s, ArCl*P*N(*i*-amyl)*P*ArCl); 54 (d, $^2J_{PP}$ = 330 Hz, Ar_2PN(*i*-amyl)PArCl), 141 (d, Ar_2PN(*i*-amyl)*P*ArCl).

Cr(CO)$_4$(PNP^{OMe}) (16). A toluene solution (30 mL) of $Cr(CO)_6$ (0.468 g, 2.12 mmol, 1 equiv) and PNP^{OMe} (1.13 g, 2.12 mmol, 1 equiv) was stirred at 110 °C in a sealed Schlenk tube for 36 h. The color of the solution gradually changed from colorless to bright yellow. Volatile materials were removed in vacuo. The yellow residue was dissolved in CH_2Cl_2 and filtered to remove a brown impurity. Upon cooling to −35 °C crystallization occurred. The mother liquor was decanted, and the residue was dried in vacuo to provide 1.166 g (1.68 mmol, 80% yield) of crystalline yellow product in two crops. ^{1}H NMR (300 MHz, $CDCl_3$) δ: 2.86 (t, $^3J_{HP}$ = 8.7 Hz, 3H, NCH_3), 3.47 (s, 12H, OCH_3), 6.85 and 7.65 (app dd, 8H, 3- and 6-aryl-*H*), 7.02 and 7.40 (app td, 8H, 4- and 5-aryl-*H*). ^{13}C NMR (75 MHz, $CDCl_3$) δ: 37.1 (t, $^2J_{CP}$ = 6.8 Hz, NCH_3), 55.1 (s, OCH_3), 110, (s, aryl), 120.5 (app t, aryl), 125.8 (app t, aryl), 131.8 (s, aryl), 133.2 (app t, aryl), 160.0 (s, aryl), 222.4 (t, $^2J_{CP}$ = 13.4 Hz, *C*O), 229.8 (app t, $^2J_{CP}$ = 9.1 Hz, *C*O). ^{31}P NMR (121 MHz, $CDCl_3$) δ: 102.6. ν_{CO} (cm^{-1}, KBr plates, CH_2Cl_2 solution): 1867, 1886, 1906, 2002. Anal. Calcd for $C_{33}H_{31}NO_8P_2Cr{\cdot}CH_2Cl_2$ (%): C, 53.14; H, 4.29; N, 1.82. Found: C, 53.64; H, 4.65; N, 1.74.

Cr(CO)$_4${NMe(PPh$_2$)$_2$} (17). A procedure similar to the one used for the preparation of **16** was employed. Yield: 54%. ^{1}H NMR (300 MHz, C_6D_6) δ: 2.32 (t, $^3J_{HP}$ = 8.4 Hz, 3H, NCH_3), 7.02 and 7.47 (m, 20H, aryl-*H*). ^{13}C NMR (75 MHz, C_6D_6) δ: 33.8 (t, $^2J_{CP}$ = 6.1 Hz, NCH_3), 129.2 (t, aryl), 131.1 (s, aryl), 132.4 (t, aryl), 137.3 (app t, aryl), 223.1 (t, $^2J_{CP}$ = 12.9 Hz, *C*O), 229.1 (t, $^2J_{CP}$ = 9.5 Hz, *C*O). ^{31}P NMR (121 MHz, C_6D_6) δ: 114. ν_{CO} (cm^{-1}, KBr plates, CH_2Cl_2 solution): ∼1881 (shoulder), 1895, 1917, 2008. Anal. Calcd for $C_{29}H_{25}NO_4P_2Cr$ (%): C, 61.82; H, 4.11; N, 2.49. Found: C, 62.79; H, 4.30; N, 2.39.

Oxidation of 16: General Procedure. Dichloromethane solutions of oxidant (I_2, Br_2, or $C_6H_5ICl_2$, 1−1.6 equiv) were added dropwise to dichloromethane solutions of yellow **16** (1 equiv) and stirred from 15 min to 6 h. The color of the reaction mixture changed upon addition to bright green (for Br_2) or dark blue ($PhICl_2$). When the oxidation was performed with I_2 (red), the color of the mixture changed slightly, to red-brown. In some cases gas evolution was observed. Generally, the ^{2}H NMR spectra of the reaction mixtures display a broad peak downfield from the diamagnetic region and some diamagnetic peaks. Recrystallization

(41) Pangborn, A. B.; Giardello, M. A.; Grubbs, R. H.; Rosen, R. K.; Timmers, F. J. *Organometallics* **1996**, *15*, 1518.

(42) Cooley, N. A.; Green, S. M.; Wass, D. F.; Heslop, K.; Orpen, A. G.; Pringle, P. G. *Organometallics* **2001**, *20*, 4769.

Table 4. Crystal and Refinement Data for Complexes 16, 18, 20, 22, and 23

	16	18	20	22	23
empirical formula	$C_{33}H_{31}NO_8P_2Cr{\cdot}C_4H_8O$	$C_{29}H_{31}Cl_3NO_4P_2Cr{\cdot}CH_2Cl_2$	$C_{29}H_{31}NO_4P_2I_3Cr{\cdot}CH_2Cl_2$	$C_{30}H_{34}Cl_2NO_4P_2Cr{\cdot}CH_2Cl_2$	$C_{41}H_{39}NO_4P_2BrCr{\cdot}CH_2Cl_2$
fw	755.63	762.76	1037.11	742.35	888.51
T (K)	98(2)	98(2)	98(2)	100(2)	98(2)
a, Å	11.7105(5)	10.6977(7)	13.5277(3)	9.7683(6)	9.9167(6)
b, Å	16.3059(8)	15.0041(10)	13.5151(3)	16.6273(10)	11.9935(8)
c, Å	19.3321(9)	21.4755(14)	20.3801(5)	20.9934(13)	17.9725(11)
α, deg					77.371(1)
β, deg	102.333(1)	96.172(1)	107.892(1)	94.990(1)°	76.328(1)
γ, deg					70.670(1)
volume, Å^3	3606.3(3)	3427.0(4)	3545.85(14)	3396.8(4)	1936.8(2)
Z	4	4	4	4	2
cryst syst	monoclinic	monoclinic	monoclinic	monoclinic	triclinic
space group	$P2_1/n$ (# 14)	$P2_1/n$ (# 14)	$P2_1/n$ (# 14)	$P2_1/c$ (# 14)	$P\bar{1}$ (# 2)
d_{calc}, g/cm^3	1.392	1.478	1.943	1.452	1.524
θ range, deg	1.65 to 28.43	1.66 to 28.17	1.61 to 35.00	1.56 to 28.33	1.82 to 28.29
μ, mm^{-1}	0.462	0.853	3.211	0.782	1.592
abs corr	none	none	none	none	none
GOF	1.755	1.579	1.405	2.760	1.731
R_1,[a] wR_2[b] [$I > 2\sigma(I)$]	0.0394, 0.0620	0.0370, 0.0621	0.0335, 0.0499	0.0618, 0.0988	0.0416, 0.0744

[a] $R_1 = \sum||F_o| - |F_c||/\sum|F_o|$. [b] $wR_2 = [\sum[w(F_o^2 - F_c^2)^2]/\sum[w(F_o^2)^2]]^{1/2}$.

from CH_2Cl_2 at −35° C followed by collection on a sintered glass funnel provided pure products according to ^{2}H NMR spectroscopy.

Compound 19: 50% yield. ^{2}H NMR (76 MHz, CH_2Cl_2) δ: 9.6 (br s, OCD_3). $\mu_{eff} = 3.6\ \mu_B$. λ_{max} (CH_2Cl_2, nm): ∼550 (br shoulder, $\epsilon = 361\ M^{-1}\ cm^{-1}$), 665 ($\epsilon = 681\ M^{-1}\ cm^{-1}$). Anal. Calcd for $C_{29}H_{19}D_{12}Br_3NO_4P_2Cr{\cdot}CH_2Cl_2$ (%): C, 39.67; H, 3.63; N, 1.54. Found: C, 40.11; H, 3.82; N, 2.21.

Compound 20: 37% yield. ^{2}H NMR (76 MHz, CH_2Cl_2) δ: 9.0 (br s, OCD_3). $\mu_{eff} = 3.6\ \mu_B$. λ_{max} (CH_2Cl_2, nm): 381 (shoulder, $\epsilon = 8100\ M^{-1}\ cm^{-1}$), 679 ($\epsilon = 953\ M^{-1}\ cm^{-1}$). Anal. Calcd for $C_{29}H_{19}D_{12}I_3NO_4P_2Cr{\cdot}CH_2Cl_2$ (%): C, 34.34; H, 3.14; N, 1.33. Found: C, 34.57; H, 3.42; N, 1.33.

$CrCl_3$(PNP^{OMe}) (18). A dichloromethane solution (20 mL) of $CrCl_3(THF)_3$ (1.513 g, 2.9 mmol, 1 equiv) was added to a solution of **1** (1.098 g, 2.9 mmol, 1 equiv) in dichloromethane (30 mL). The color of the reaction mixture turned from purple to blue within 5 min of stirring. The reaction mixture was stirred for 1 h. Volatile materials were removed in vacuo, and the blue residue was triturated three times with dichloromethane. The resulting solid was suspended in dichloromethane and stored at −35° C overnight. The desired product was collected as a bright blue powder by filtration through a sintered glass frit, washed with dichloromethane, and dried under vacuum. The filtrate contained one or two unidentified paramagnetic species, displaying peaks at 4.85 and 9.5 ppm in the ^{2}H NMR spectrum. Compound **18** obtained in this manner amounted to 1.188 g (53% yield). ^{2}H NMR (76 MHz, CH_2Cl_2) δ: 8.8 (br s, OCD_3); at 40 °C: 8.4 (br s); at −60 °C: 3.8 (br s), 32 (v br s). Coalescence temperatures (°C): −50, −10. $\mu_{eff} = 3.8\ \mu_B$. λ_{max} (CH_2Cl_2, nm): 536 ($\epsilon = 269\ M^{-1}\ cm^{-1}$), 661 ($\epsilon = 484\ M^{-1}\ cm^{-1}$). Anal. Calcd for $C_{29}H_{31}Cl_3NO_4P_2Cr{\cdot}CH_2Cl_2$ (%): C, 47.23; H, 4.32; N, 1.84. Found: C, 46.24; H, 4.29; N, 1.77.

$CrCl_3$(P^{t-Bu}N^{i-amyl}P^{OMe}) (21). A procedure similar to the one used for the preparation of **18** was employed. Recrystallization from a CH_2Cl_2 solution layered with petroleum ether afforded the desired product as a purple powder in 75% yield. ^{2}H NMR (76 MHz, CH_2Cl_2) δ: 7 (v br, OCD_3); at 40 °C: 7.1 (br s); at −90 °C: 4.4 (br s), 28 (v br s). Coalescence temperatures (°C): −5, 18. $\mu_{eff} = 3.9\ \mu_B$. λ_{max} (CH_2Cl_2, nm): 517 ($\epsilon = 250\ M^{-1}\ cm^{-1}$), 663 ($\epsilon = 498\ M^{-1}\ cm^{-1}$). Anal. Calcd for $C_{49}H_{59}D_{12}Cl_3NO_4P_2Cr{\cdot}CH_2Cl_2$ (%): C, 59.35; H, 7.21; N, 1.38. Found: C, 59.76; H, 7.63; N, 1.34.

$CrCl_2(CH_3)$(PNP^{OMe}) (22). A dichloromethane solution of PNP^{OMe} (105 mg, 0.20 mmol, 1 equiv) was added to a dichloromethane solution of $CrCl_2(CH_3)(THF)_3$ (70 mg, 0.20 mmol, 1 equiv) to generate a brown-green solution. The reaction mixture was stirred for 10 min, and then the volatiles were removed under vacuum. Upon concentration, the color of the solution turned olive green. The residue was dissolved in CH_2Cl_2 and layered with petroleum ether. Storing at −35 °C caused product crystallization as dark brown needles. The mother liquor was decanted, and the crystals were washed with a cold CH_2Cl_2/petroleum ether mixture. This procedure afforded 109 mg (82% yield) of desired product. ^{2}H NMR (76 MHz, CH_2Cl_2) δ: 6.3 (br s, 6D, OCD_3), 13.6 (br s, 6D, OCD_3); at −90 °C: 6.9 (br s), ∼25 (v br s); at 71° C (PhCl): 7.3 (br s). Coalescence temperatures (°C): ←80, 40. $\mu_{eff} = 3.7\ \mu_B$. λ_{max} (CH_2Cl_2, nm): 462 ($\epsilon = 495\ M^{-1}\ cm^{-1}$), 495 (($\epsilon = 379\ M^{-1}\ cm^{-1}$) shoulder), 700 ($\epsilon = 261\ M^{-1}\ cm^{-1}$). Anal. Calcd for $C_{30}H_{22}D_{12}Cl_2NO_4P_2Cr{\cdot}CH_2Cl_2$ (%): C, 49.37; H, 4.77; N, 1.85. Found: C, 48.98; H, 5.13; N, 1.76.

CrBr(*o,o′*-biphenyldiyl)(PNP^{OMe}) (23). Magnesium turnings (12.3 mg, 1.4 mmol, 8 equiv) were added to a diethyl ether solution (10 mL) of *o,o′*-dibromobiphenyl (53.5 mg, 0.17 mmol, 1 equiv) and stirred overnight at room temperature or with heating. The solution was decanted and concentrated to approximately 5 mL to cause precipitation of a white solid, which was dissolved by addition of dichloromethane. The resulting solution was cooled to almost freezing, then added to a thawing dichloromethane solution (20 mL) of **18** (0.1183 mg, 0.17 mmol, 1 equiv). The color of the reaction mixture gradually changed from dark blue to forest green upon warming. The reaction mixture was stirred for 2 h, then volatile materials were removed in vacuo. Dichloromethane was added to the green residue and the mixture filtered through Celite to remove a brown solid. The green filtrate was concentrated, layered with petroleum ether, and cooled to −35 °C to cause crystallization of **23** as a green material. The green solid was collected on a sintered glass frit, washed with cold dichloromethane, and dried under vacuum to provide 104.2 mg of desired product (0.12 mmol, 75% yield). In cases when a white powder (probably magnesium salts) precipitated out along with the desired product, an additional recrystallization provided clean product. ^{2}H NMR (76 MHz, CH_2Cl_2) δ: 5.8 (br s, OCD_3), 9 (v br s, OCD_3); at 45 °C: 7.3 (br s); at −87 °C: 2.7 (br s), 5.7 (br s), 29.2 (v br s). Coalescence temperatures (°C): −10, 15. $\mu_{eff} = 3.8\ \mu_B$. λ_{max} (CH_2Cl_2, nm): 382 ($\epsilon = 1937\ M^{-1}\ cm^{-1}$), 449 ($\epsilon = 809\ M^{-1}\ cm^{-1}$), 598 ($\epsilon = 364\ M^{-1}\ cm^{-1}$). Anal. Calcd for $C_{41}H_{39}NO_4P_2BrCr$ (%): C, 61.28; H, 4.89; N, 1.74. Found: C, 61.38; H, 4.93; N, 2.10.

Trimerization Trials with MAO Activation. A toluene solution (30 mL, 4×10^{-4} M) of a well-defined chromium(III)(PNP) complex was prepared. The mixture was cooled to −78 °C in a dry ice/acetone bath and degassed, then allowed to warm to room temperature. The solution was magnetically stirred under ethylene, and MAO (10% in toluene, 300 equiv) was added via syringe. Ethylene consumption was monitored by noting the decrease in pressure in the system over time (the pressure was kept between 771 and 655 Torr), and 1-hexene formation was documented by

GC and GC-MS. For 1 h runs, the reaction produces 1-hexene with a range of 1900−2800 turnovers in greater than 80% overall selectivity for **18**; 300−600 turnovers in greater than 90% overall selectivity for **23**; and 1300−2000 turnovers in greater than 70% overall selectivity for **21**. The C10 fraction is the major impurity detectable.

Trimerization of Ethylene with 23 upon Halide Abstraction. Dichloromethane-d_2 was vacuum transferred to a J-Young tube or Schlenk flask charged with **23** (8−34 mg, 10−42 μmol, 1 equiv) and $NaB[C_6H_3(CF_3)_2]_4$ (10.5−45 mg, 12−51 μmol, 1.2 equiv). The mixture was warmed to room temperature using a water bath followed by mixing (via mechanical rotation for NMR tubes or magnetic stirring for flasks) for 10 min. The mixture turned brown as the starting materials dissolved. Ethylene (128.2 mL at 30−125 Torr, 200−860 μmol, 17.5−23 equiv) was condensed in (∼2.3−3.8 atm in the vessel at room temperature). The reaction mixture was mixed for 1−1.5 h at room temperature, during which the mixture turned brown-green. *o*-Vinyl-biphenyl and 1-hexene were detected by ^{1}H NMR spectroscopy. Relative to the amount of *o*-vinyl-biphenyl observed, about 3.5 equiv of 1-hexene is formed (ca. 60%).

Reaction of 23 with Ethylene. Dichloromethane-d_2 was vacuum transferred to a J-Young tube charged with **23** (8.1 mg, 10.1 mmol, 1 equiv). Ethylene (43.48 mL at 87 Torr, 200 mmol, 20 equiv) was condensed in (∼2 atm in the tube at room temperature). The mixture was warmed to room temperature using a water bath, then mixed by mechanical rotation for 1 h. During this time the mixture achieved a brown-green color. *o*-Vinyl-biphenyl was detected by ^{1}H NMR spectroscopy, but no 1-hexene was observed. After an additional 1 h of mixing the mixture turned brown-red, but no 1-hexene was formed according to ^{1}H NMR spectroscopy.

X-ray Crystal Data: General Procedure. Crystals grown from THF (**16**) or CH_2Cl_2/petroleum ether (**18**, **20**, **22**, and **23**) at −35 °C were removed quickly from a scintillation vial to a microscope slide coated with Paratone N oil. Samples were selected and mounted on a glass fiber with Paratone N oil. Data collection was carried out on a Bruker Smart 1000 CCD diffractometer. The structures were solved by direct (**16**, **18**, **22**, and **23**) or Patterson methods (**20**) (SHELXTL-97, Sheldrick, 1990) in conjunction with standard difference Fourier techniques. All non-hydrogen atoms were refined anisotropically. Some details regarding refined data and cell parameters are available in Table 4. Selected bond distances and angles are supplied in Table 3 and in the captions of Figures 1, 2, 3, 4, and 5.

Acknowledgment. We thank Dr. Steven A. Cohen for helpful discussions. We are grateful to BP Chemicals (now Innovene) for financial support.

Supporting Information Available: Tables of bond lengths, angles, and anisotropic displacement parameters for **16**, **20**, and **22** (corresponding tables for **18** and **23** were reported previously).[23] Drawing of the solid-state structure of **21**. Plots of ethylene consumption over time with **18**, **21**, and **23** activated with MAO (PDF). X-ray crystallographic data (CIF). This material is available free of charge via the Internet at http://pubs.acs.org.

OM050605+